Histol Histopathol (2022) 37: 839-852

http://www.hh.um.es

Histology and Histopathology
From Cell Biology to Tissue Engineering

ORIGINAL ARTICLE **Open Access**

Sargassum horneri extract containing polyphenol alleviates DNCB-induced atopic dermatitis in NC/Nga mice through restoring skin barrier function

Suyama Prasansali Mihindukulasooriya[1]*, Duong Thi Thuy Dinh[1]*, Kalahe Hewage Iresha Nadeeka Madushani Herath[1,2,3], Hyo Jin Kim[4], Eui-Jeong Han[5], Jinhee Cho[2], Mi-Ok Ko[2], You-Jin Jeon[6], Ginnae Ahn[5] and Youngheun Jee[1,2]

[1]Interdisciplinary Graduate Program in Advanced Convergence Technology and Science, [2]Department of Veterinary Medicine and Veterinary Medical Research Institute, Jeju National University, Jeju, Republic of Korea, [3]Department of Biosystems Engineering, Faculty of Agriculture and Plantation Management, Wayamba University of Sri Lanka, Makandura, Sri Lanka, [4]Department of Food Bioengineering, Jeju National University, Jeju, [5]Department of Food Technology and Nutrition, Chonnam National University, Yeosu and [6]Department of Marine Life Science, School of Marine Biomedical Sciences, Jeju National University, Jeju, Republic of Korea

*These authors equally contributed to this study

Summary. Atopic dermatitis (AD) is a chronic inflammatory skin disease characterized by skin barrier dysfunction. *Sargassum horneri* (*S. horneri*) is a brown alga that has been widely used in traditional medicine of eastern Asian countries. Recent studies proved that a brown alga *S. horneri* has anti-inflammatory activity. In this study, we investigated the effect of *S. horneri* ethanol extract (SHE) against AD in 2,4-dinitrobenzene (DNCB) induced AD in NC/Nga mice. We observed that SHE treatment decreased the epidermal thickness and epidermal hyperplasia that had been worsened through DNCB application. Moreover, SHE significantly inhibited the proliferation of mast cells and decreased the expression of IL-13 on $CD4^+$ cells prompted by elevated thymic stromal lymphopoietin (TSLP) expression in DNCB-induced AD in mice. We also demonstrated that SHE directly inhibited the expression of keratinocyte-produced TSLP known to exacerbate skin barrier impairment. Especially, the decrease of filaggrin, an integral component of proper skin barrier function through a function in aggregating keratin filaments, observed in DNCB-induced AD mice was significantly improved when treated with SHE. More importantly, we proved that SHE was able to decrease the serum levels of IgG_1 and IgG_{2a}, two crucial factors of AD, indicating the protective effect of SHE. Taken together, our findings suggest that SHE may protect NC/Nga mice against DNCB-induced AD via promoting skin barrier function.

Key words: Brown alga, Thymic stromal lymphopoietin (TSLP), Filaggrin, Skin barrier

Corresponding Author: Youngheun Jee, Department of Veterinary Medicine and Veterinary Medical Research Institute, Jeju National University, Jeju 63243, Republic of Korea. e-mail: yhjee@jejunu.ac.kr

DOI: 10.14670/HH-18-473

Introduction

Atopic dermatitis (AD) is a chronic inflammatory skin disease and has a major detrimental impact on patients' quality of life when developed due to its symptoms like dry, red, cracked, and pruritic skin (Bieber, 2010). The prevalence of AD is 10–20% in children and 1–3% in adults, and its incidence has increased two to three folds during the past three decades (Kolb and Ferrer-Bruker, 2020). Although the cause of this disease is not known for sure, genetic changes, immune system dysfunction, and increased exposure to environmental substances such as tobacco smoke, skin products, soaps, and air pollutants are suspected as potential sources (Kantor and Silverberg, 2017).

Prolonged tissue inflammation and epidermal barrier dysfunction are hallmark features of AD. As an efficient physical, chemical, microbial, and immunological barrier, skin performs various protective functions. In particular, the skin barrier in epidermis plays a key role

Abbreviations. AD, Atopic dermatitis; DNCB, 2,4 dinitrobenzene; HDM, House dust mites; HRP, Horseradish peroxidase; IFN, Interferon; IgG, Immunoglobulin; IL, Interleukin; SDS, Sodium dodecyl sulfate; SHE, Sargassum horneri extract; TNF, Tumor necrosis factor; TSLP, Thymic stromal lymphopoietin

in immune surveillance and homeostasis, and in preventing the penetration of microbial products and allergens.

Proper maintenance of skin epidermis requires uninterrupted formation of an impermeable skin barrier through a controlled progression of cellular cycles like proliferation, differentiation, and death in skin epidermis, and it is well known that specific proteins including filaggrin, loricrin, and involucrin are required to cross link cells in an intricate manner (Kim et al., 2012). Filaggrin, in particular, seems to perform a crucial role in AD as the encoded protein is involved in aggregating keratin filaments and hence aids the formation and maintenance of the epidermal barrier.

Filaggrin is a protein produced by keratinocytes. It is the main component of keratohyalin granules whose contents are discharged during skin cell differentiation. Changes in skin barrier due to filaggrin deficiency weakens its protective function and may lead to more inflammation by allowing more allergens to penetrate through the less compacted epidermal matrix (De Vuyst et al., 2017). Therefore, factors influencing filaggrin balance in skin are of utmost importance in AD.

Thymic stromal lymphopoietin (TSLP), a master regulator of Th2-driven inflammation is identified as being elevated in AD patients' skins, and is known to influence keratinocyte function and skin barrier integrity by modulating the Th2 immune reaction (Ray et al., 1996). The skin lesions of AD subsequently exhibit deviated Th2 immune reactions, and the deviation widens progressively as the disease manifests chronicity. Th2 cytokines further deteriorate the skin barrier function by inhibiting filaggrin expression. For instance, interleukins (IL) such as IL-4 and IL-13, detected to be promoted in AD lesions, also lead to decreased expression of filaggrin in keratinocytes. TSLP also activates dendritic cells, which in turn modulates T cell functions and further disrupts balanced Th2 immune reaction. Moreover, immunoglobulins are involved in a number of immune response pathways in AD, and Th2 cells or mast cells are known to stimulate the secretion of IgG_1 in B cells while Th1 cells might trigger the secretion of IgG_{2a} in mice (Lee et al., 2010). Therefore, comparison of serum IgG_1 and IgG_{2a} can be an important marker representing Th1/Th2 balance in AD.

Marine algae with abundant polysaccharides and polyphenols are beneficial for human health and have been traditionally used as anti-inflammatory drugs in Asian countries (Wijesinghe and Jeong, 2011; Jeong et al., 2014). For instance, *S. horneri*, an edible brown seaweed distributed mostly in coastal areas of Korea, Japan and China, has been a fundamental source of food and drug for centuries (Zheng et al., 2009). Recently, through a series of studies, we have elucidated numerous fundamental and health beneficial anti-inflammatory and antioxidant characteristics of it. We found that *S. horneri* contains a great amount of nutrients like dietary fibers, vitamins, amino acids, and polysaccharides as well as polyphenols and polysaccharides (Kim et al., 2018a; Herath et al., 2019). Moreover, we found that extracts of *S. horneri* have bioactive properties such as antioxidant and anti-cancer *in vitro* (Sanjeewa et al., 2019). We showed the suppressive effect of *S. horneri* ethanol extract (SHE) on Concanavalin A induced activation of immune cells such as granulocytes, eosinophils, T cells, and monocytes in murine splenocytes (Herath et al., 2019). We also showed the anti-inflammatory effect of the sulfated polysaccharides of *S. horneri* in RAW 264.7 cells, which works via inhibiting the inducible nitric oxide synthase (iNOS) and cyclooxygenase (COX)-2 expression by lowering nuclear factor (NF)-kB (Sanjeewa et al., 2019). Though not our own research, sargachromanol, a chrome compound isolated from *S. horneri*, was also shown to protect skin damage induced by ultraviolet A in NC/Nga mice (Kim et al., 2012).

These studies clearly indicate that SHEs, rich in sulfated polysaccharides, have an anti-inflammatory capacity in a wide variety of biological systems and diseases (Zheng et al., 2009). In contrast, however, few studies so far have investigated the anti-inflammatory activity of *S. horneri* against AD, one of the archetypal biological systems implicated by protracted inflammation in skin. In the current study, we investigated the preventive therapeutic effects of an SHE in DNCB-induced AD in NC/Nga mice, particularly focusing on its potential to recover the function of skin barrier. We examined molecular factors known to affect filaggrin expression such as pro-inflammatory Th2 cytokines, TSLP, etc.

Materials and methods

Preparation of SHE

S. horneri obtained from coastal areas of Jeju, South Korea, was prepared as previously described (Herath et al., 2021). In brief, the powdered seaweed (100 g) was dissolved in 2 L ethanol for 12 h. The solution was centrifuged at 12,000 rpm at room temperature after clay treatment and concentrated to 20% of the solid concentration. Finally, the sample was freeze dried and stored at -20°C until use. The total polyphenol content of resultant SHE was 67.58 mg of gallic acid equivalents (GAE)/g, and gallic acid content was quantified to 8.26 mg/g (Herath et al., 2021).

Animals

8 weeks old female NC/Nga mice were purchased from Orient Bio (Gwangju, Korea) and housed in ventilated cages under pathogen-free conditions at constant temperature 23 ± 1.5°C and 55 ± 15% humidity with a 12 h light-dark cycle. Mice were fed with approved diet and water ad libitum. All experimental protocols were approved by the Institutional Animal Care and Use Committee of Chonnam National University (No.CNU IACUC-YS-2016-6).

Animal model

To induce experimental AD skin lesions, we first shaved the dorsal hair of NC/Nga mice using an electric shaver and applied a hair removal cream and sodium dodecyl sulfate (SDS) to the shaved skin areas 3 h before applying house dust mites (HDM) DNCB and AD cream (Biostir-AD, Biostir, Kobe, Japan). The induction of AD to shaved dorsal skin areas were designed as shown schematically in Fig. 1. Mice were randomized into naïve (n=8) where mice were left untreated with any of DNCB, SHE, CJLP133 during the whole course of experimental time frame and the experimental group where mice were all applied with DNCB in the shaved skin area first. Then, at day 14 after the first application of DNCB, mice in the experimental group were further randomized into four groups, DNCB (n=8), DNCB+SHE10 (n=8), DNCB+SHE100 (n=8), and DNCB+CJLP133 (a positive control group, n=8), and treated as follows: mice in DNCB group were applied 0.5% DNCB twice every week (Fig. 1); those in DNCB+SHE10 and DNCB+SHE100 were administered SHE 10 mg/kg and 100 mg/kg suspended in saline orally, respectively, every day besides DNCB application; those in DNCB+CJLP133 were administered CJLP133, Lactobacillus plantarum of proven therapeutic efficacy against AD, orally every day besides DNCB application and treated as the positive control in this study.

Histopathological Analysis

Skin tissues were fixed in 10% formalin and embedded in paraffin. Sections of 3 μm thickness were cut and stained with hematoxylin-eosin (H&E) to assess the histopathological changes and to measure epidermal thickness. Mast cells were stained in 0.5% Toluidine blue (Sigma-Aldrich) to monitor the distribution and degranulation patterns of mast cells in dermis. Stained sections were dehydrated in a series of ethanol and cleared in xylene. Each section was observed using an Olympus DP-72 microscope camera (Olympus, Tokyo, Japan).

Immunohistochemestry staining

Immunohistochemistry staining was performed on formalin–fixed, paraffin–embedded skin tissue sections by using horseradish peroxidase (HRP)-labeled Vectastain Elite ABC kit (Vector) according to manufacturer's instructions. Sections were deparaffinized and rehydrated through a graded series of ethanol. Recaptured tissues were immersed in 0.3% hydrogen peroxide for 30 min followed by incubation with blocking serum (Vector Laboratories) to prevent nonspecific binding. The tissues were incubated overnight at 4oC with antibodies against anti-Ki67 (1:400, Abcam) and filaggrin (1:400, BioLegends). After washing, tissues were incubated with biotinylated secondary antibody solution for 45 min. Phosphate buffer solution (PBS) was used to wash the incubated tissues, and subsequently a solution containing avidine:biotine peroxidase complex was applied to the sections for 45 min. Diaminobenzidine (DAB, Vector Laboratories) was used to visualize the immuno-reactivity and counterstained with hematoxylin (Dako). Images were collected using a microscope (Olympus, Tokyo, Japan), and positive cells were quantified using ImageJ software (v1.46; National Institute of Health, Bethesda, Maryland, USA).

Double immunofluorescence staining

For the detection of IL-13 expression in skin tissues, immunofluorescence double-labeling was performed. Sections were incubated with primary antibodies of IL-13 (1:200, Santa Cruz Biotechnology) together with those of CD4 (1:200, Novus Biologicals) followed by appropriate secondary antibodies of FITC anti-mouse (1:100, Santa Cruz Biotechnology) and STAV-TRITC (1:200, Zymed Laboratories, Carlton court, USA), respectively. To determine the expression of TSLP in skin tissues, they were incubated with primary antibodies of TSLP (1:800, Novus Biologicals) together with those of Ki-67 (1:400, Abcam) followed by secondary antibodies directly conjugated with Alexa Fluor 488 at dilution 1:200 and STAV-TRITC (1:200, Zymed Laboratories, Carlton court, USA), respectively. And they were counterstained with 4', 6-diamino-2-phenylindole dihydrochloride (DAPI, 1:2000, Sigma Aldrich) and observed under a fluorescent microscope (Leica DM LB2, Leica) with appropriate filters.

Real-time polymerase chain reaction (RT-PCR) analysis in the skin

Quantification of the mRNA expression of IL-13 and TSLP was performed by using RT-PCR. Total RNA in skin tissue was isolated using Trizol reagent. Then the PCR was carried out according to the following program: 35 cycles of 5 min denaturation at 94°C, followed by 1 min annealing at 55-60°C, and then 20 min extension at 72°C on a StepOnePlus real-time PCR system (Applied Biosystem, Foster City, CA). The fold changes in expression were calculated using the $2^{\Delta\Delta CT}$ method using endogenous control. GAPDH was used for normalization. We listed the primer sequences in Table 1.

ELISA assay for IgG_1 and IgG_{2a} measurement

ELISA kits were separately used to measure the serum IgG_1 and IgG_{2a} levels. The collected serum from NC/Nga mice was poured into specific antigen coated microplate wells. Serum samples were incubated at room temperature for about 1 h with captured antibodies. After that, blocking solution was added to avoid non-specific bindings. Microplates were washed and treated with horseradish peroxidase (HRP) detection antibody and

then 3,3',5,5'- tetramethylbenzidine (TMB) substrate was added. Absorbance was measured using Multi-Microplate Reader (Bio-Health Materials Core-Facility, Jeju National University), and concentrations of IgG_1 and IgG_{2a} were estimated according to the standards in manufacturer's instructions.

Statistical Analysis

Numerical data are presented as means ± S.E.M. for respective groups. Statistical analysis was performed by using analysis of variance (ANOVA) followed by Bonferroni post hoc test. $P<0.05$ was considered significant in this study.

Results

SHE reduced the epidermal thickness and hyperplasia in the skin of DNCB-induced AD mice

We have determined the histopathological changes that occurred in skins of DNCB-induced AD NC/Nga mice. As observed in Fig. 2K, the thickness of stratum corneum of skin was significantly increased when DNCB was applied and AD was developed (Fig. 2B) compared to that in the naïve group (Fig. 2A; $p<0.0005$). However, SHE treatment with 10 and 100 mg/kg concentrations reduced the thickness of stratum corneum in DNCB-induced AD mice significantly by 2.2 folds ($p<0.0005$; Fig. 2C) and 1.9 folds ($p<0.005$; Fig. 2D), respectively. Interestingly, both SHE concentrations were similarly effective as the positive control CJLP-133 where the thickness of stratum corneum shrank by 2 folds ($p<0.05$; Fig. 2E).

Besides, skin epidermal thickness was also increased in the DNCB group (Fig. 2G) as compared with that in the naïve group (Fig. 2F; $p<0.005$). Moreover, SHE similarly decreased the dermatitis thickness of DNCB-induced skin lesions in a dose-dependent manner. As shown in Fig. 2L, the epidermis thickness was reduced by 1.2 (Fig. 2H) and 1.6 folds ($p < 0.05$; Fig. 2I) when treated with 10 and 100 mg/kg of SHE, respectively. Especially, in decreasing the thickness of epidermis, SHE 100 mg/kg was as effective as CJLP-133 (Fig. 2J) where the epidermis thickness shrank by 1.7 folds ($p<0.05$).

To account for epidermal changes of DNCB-induced AD skins, the level of epidermal hyperplasia was assessed using the number of Ki-67 positive cells in the basal layer of epidermis. As expected, a significantly increased number of positive cells were observed in the DNCB group (Fig. 3B) compared to those in the naïve group (Fig. 3A) in skin tissues ($p<0.0005$; Fig. 3F). However, as shown in Fig. 3F, the number of positive cells in DNCB+SHE10 and DNCB+SHE100 ($p<0.05$) groups was lower than that in DNCB. In particular, SHE 100 mg/kg was more effective than the positive control CJLP-133 (Fig. 3E) in reducing the number of Ki-67 positive cells.

Taken together, these results suggest that epidermal thickness, and epidermal hyperplasia in skin tissues increase when DNCB is applied and AD is developed in NC/Nga mice, but SHE treatment might attenuate those symptoms significantly.

SHE prevented mast cell infiltration and degranulation in the skin of DNCB-induced AD mice

Toluidine blue staining of skin tissue sections was used to reveal the mast cell infiltration into dermis of NC/Nga mice. As shown in Fig. 4K, the infiltration of mast cells was significantly increased in the DNCB group as compared to that in the naïve group ($p<0.0005$, Fig. 4A,B). By contrast, SHE 10 mg/kg and SHE 100 mg/kg (Fig. 4C,D) were as effective as the positive

Table 1. RT-PCR Primers.

Primers	Sequences
IL-13	Forward: CAA TTG CAA TGC CAT CTA CAG GAC Reverse: CGA AAC AGT TGC TTT GTG TAG CTGA
TSLP	Forward: TAT GAG TGG GAC CAA AAG TAC CG Reverse : GGG ATT GAA GGT TAG GCT CTG G
GAPDH	Forward: CAT CCG TAA AGA CCT CTA GCC AAC Reverse: ATG GAG CCA CCG ATC CAC A

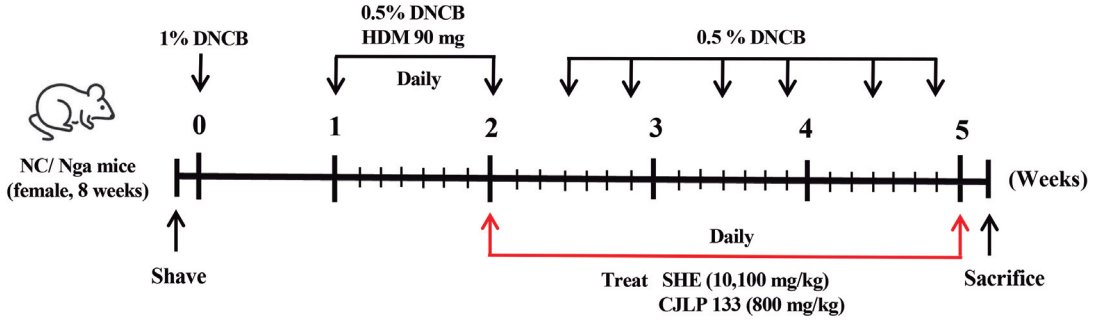

Fig. 1. Mouse model of DNCB-induced atopic dermatitis. Mice were divided into five groups as naïve (control), DNCB group (HDM/DNCB applied mice), DNCB+SHE10 group (HDM/DNCB and SHE (10 mg/kg) co-applied mice), DNCB+SHE100 groups (HDM/DNCB and SHE (100 mg/kg) co-applied mice), and DNCB+CJLP133 group (a positive control group with HDM/DNCB and CJLP 133 (800 mg/kg) co-applied mice). Respective administration/treatment schedules are schematically illustrated.

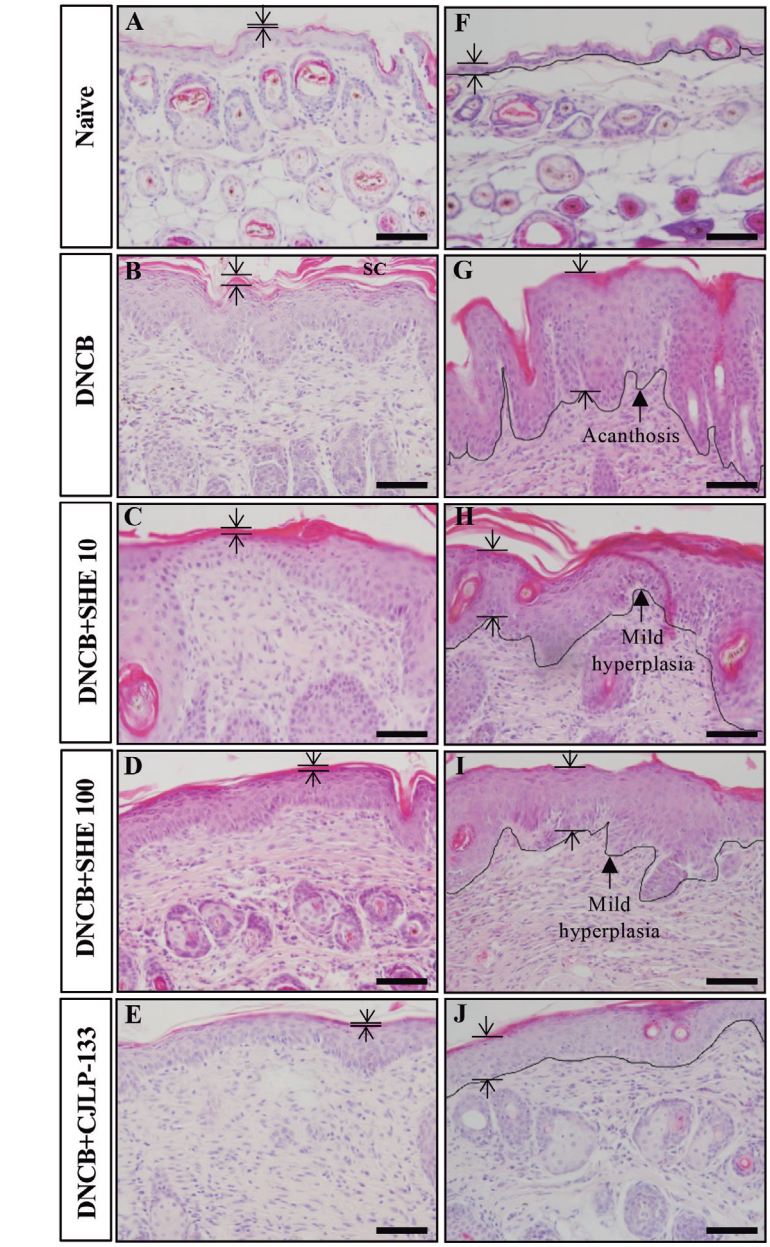

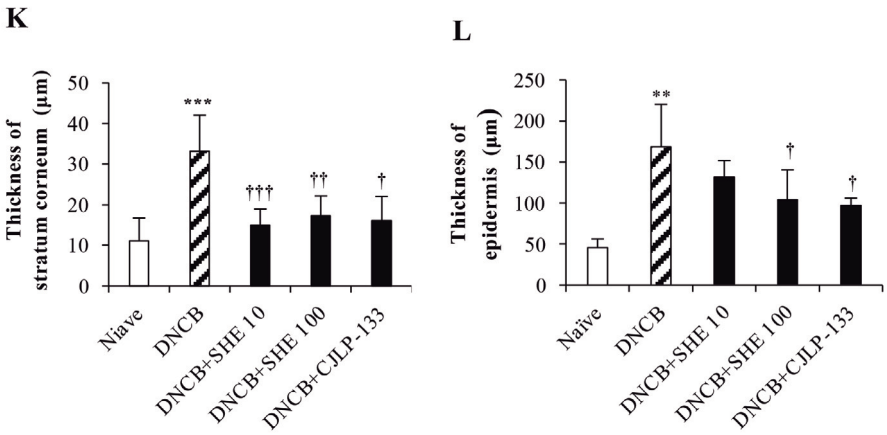

Fig. 2. SHE shrinks the expanded thicknesses of epidermal and stratum corneum of the skin on DNCB-induced AD mice. **A-J.** Representative images of skin sections stained with H&E are shown. The thickness of the stratum corneum is marked in **(A-E)** while epidermal thickness is indicated in **(F-J)**. "SC" in **(B)** depicts the stratum corneum (Pasonen-Seppänen et al., 2001). Pathologic lesions are marked by thick arrows in **(G-I)**. Black lines in **(F-J)** indicate the boundary between epidermal and dermal layers. The thicknesses of **(K)** skin stratum corneum and **(L)** skin epidermis are displayed. Data are presented as the mean ± SE of changes in values. * ($p<0.05$), ** ($p<0.005$) and *** ($p<0.0005$) indicate significant increases compared to the naïve group, and † ($p<0.05$), †† ($p<0.005$) and ††† ($p<0.0005$) represent significant decreases compared to the DNCB group, respectively. Scale bars: 25 μm.

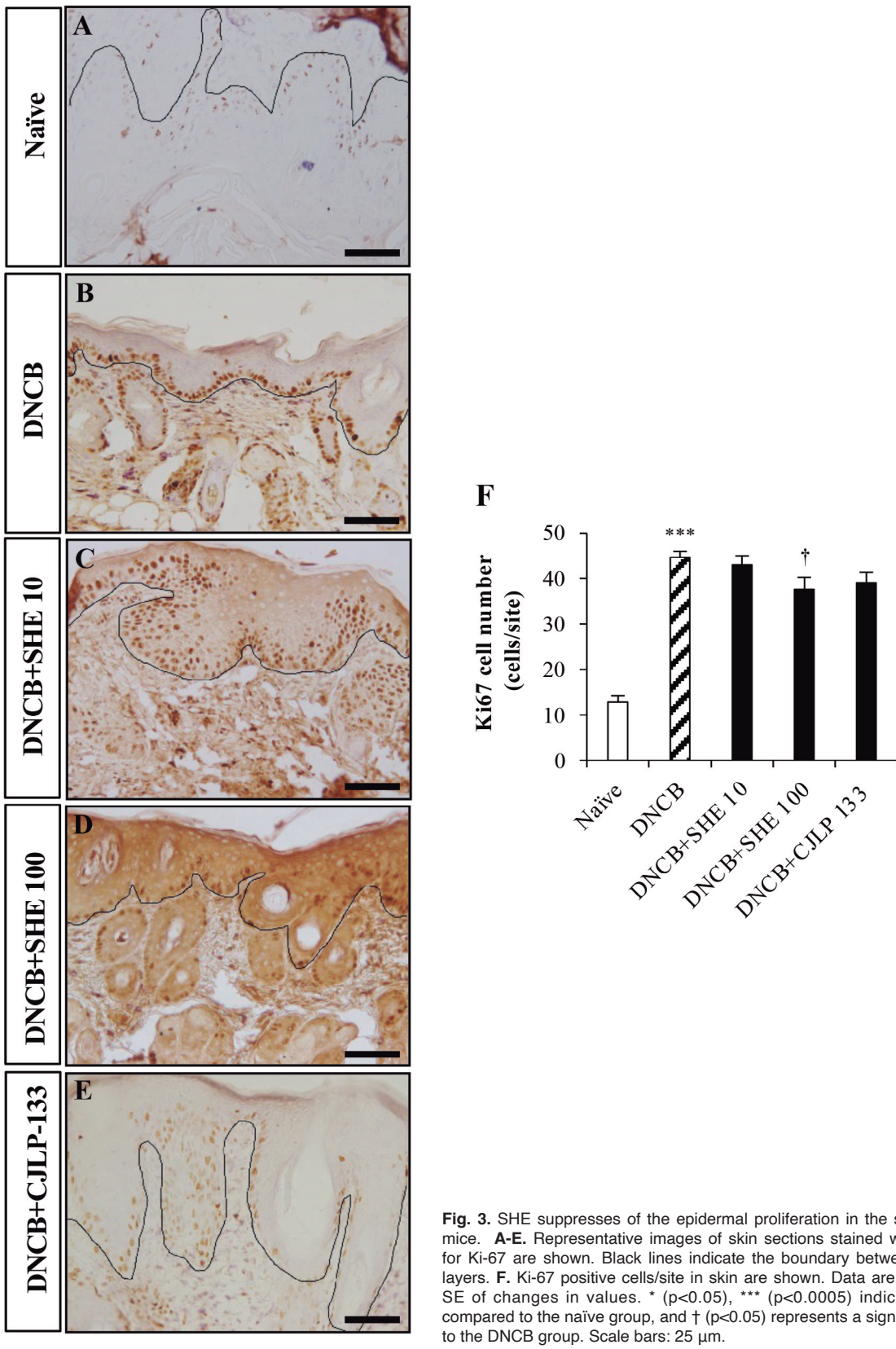

Fig. 3. SHE suppresses of the epidermal proliferation in the skin of DNCB-induced AD mice. **A-E.** Representative images of skin sections stained with immunohistochemistry for Ki-67 are shown. Black lines indicate the boundary between epidermal and dermal layers. **F.** Ki-67 positive cells/site in skin are shown. Data are presented as the mean ± SE of changes in values. * ($p<0.05$), *** ($p<0.0005$) indicate significant increases compared to the naïve group, and † ($p<0.05$) represents a significant decrease compared to the DNCB group. Scale bars: 25 μm.

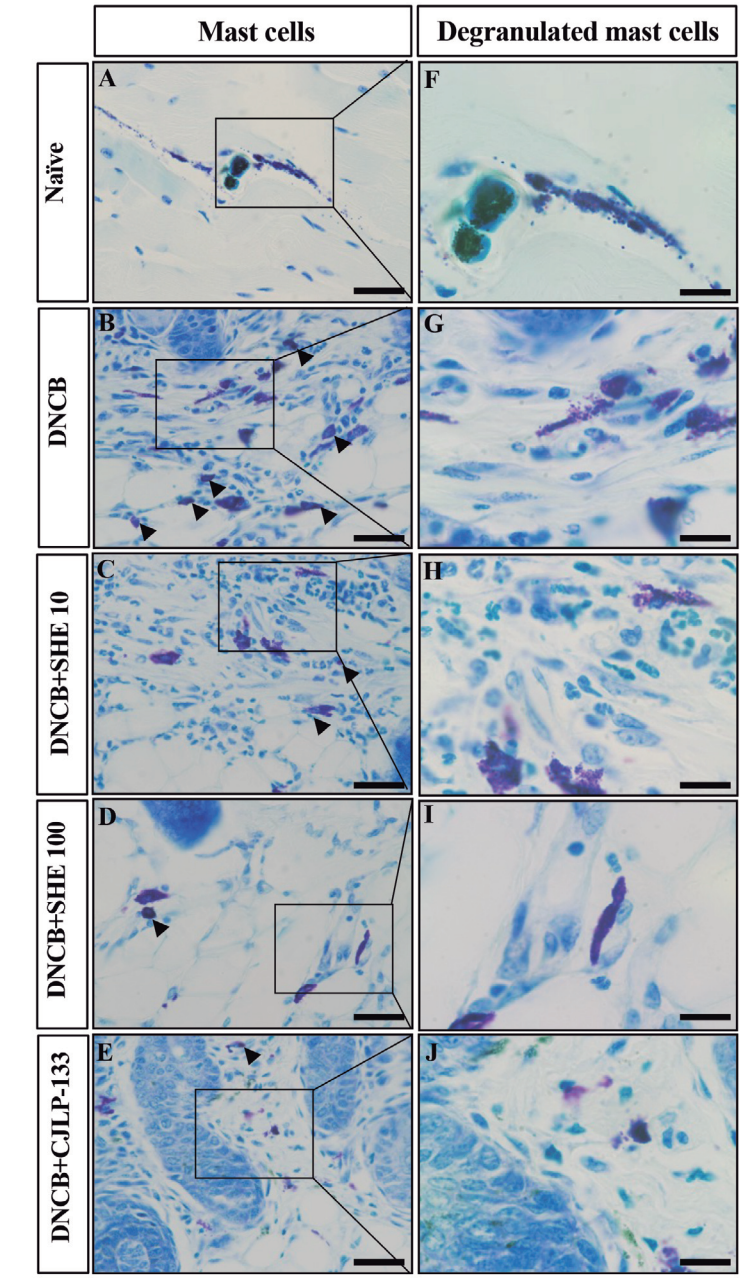

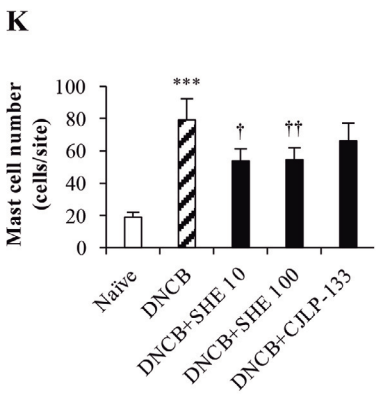

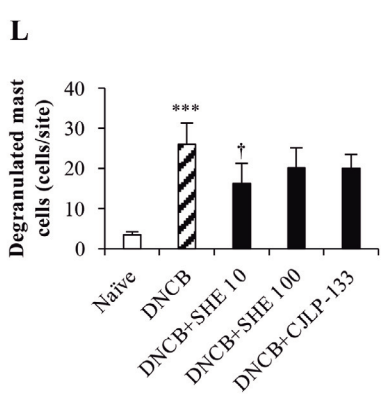

Fig. 4. SHE inhibits mast cell infiltration and degranulation activated in the skin of DNCB-induced AD mice. **A-J.** Representative images of mast cell infiltration and degranulated mast cells in skin are shown. **K.** Number of mast cells infiltrated in skin and **(L)** degranulated mast cells/site in skin. Mast cells, indicated by black arrow heads, can be found as purple dense granules while degranulated mast cells are located inside designated areas of **(A-E)** whose magnification in **(F-J)** reveals degranuated mast cells clearly. Data are presented as the mean ± SE of changes in values. *** ($p<0.0005$) indicates a significant increase compared to the naïve group, and † ($p<0.05$), †† ($p<0.005$) represent significant decreases compared to the DNCB group. Scale bars of **(A-E)** are 25 μm and **(F-J)** captured by an oil-immersion lens are 10 μm.

control CJLP-133 (Fig. 4E) in decreasing the infiltration of mast cells in the skin of AD mice.

Activated mast cells undergo degranulation and release histamine and other vasoactive mediators to promote subsequent inflammatory responses. When DNCB was applied to skins of NC/Nga mice, degranulation of mast cells was indeed increased by 7.4 folds ($p<0.0005$; Fig. 4G,L) compared to that in the naïve group (Fig. 4F,L). However, when DNCB-induced AD mice were treated with SHE, mast cell degranulation was significantly reduced in the skin compared to that in DNCB-induced AD mice. Specifically, the level of mast cell degranulation was decreased by 1.6 folds at 10 mg/kg ($p<0.05$; Fig. 4H,L) and by 1.3 folds at 100 mg/kg (Fig. 4I,L). Moreover, SHE treatment was more effective than or similar to the treatment with the positive control agent, CJLP-133 (Fig. 4J) in reducing the level of mast cell degranulation in DNCB-induced AD mice.

These results indicate that SHE treatment suppresses

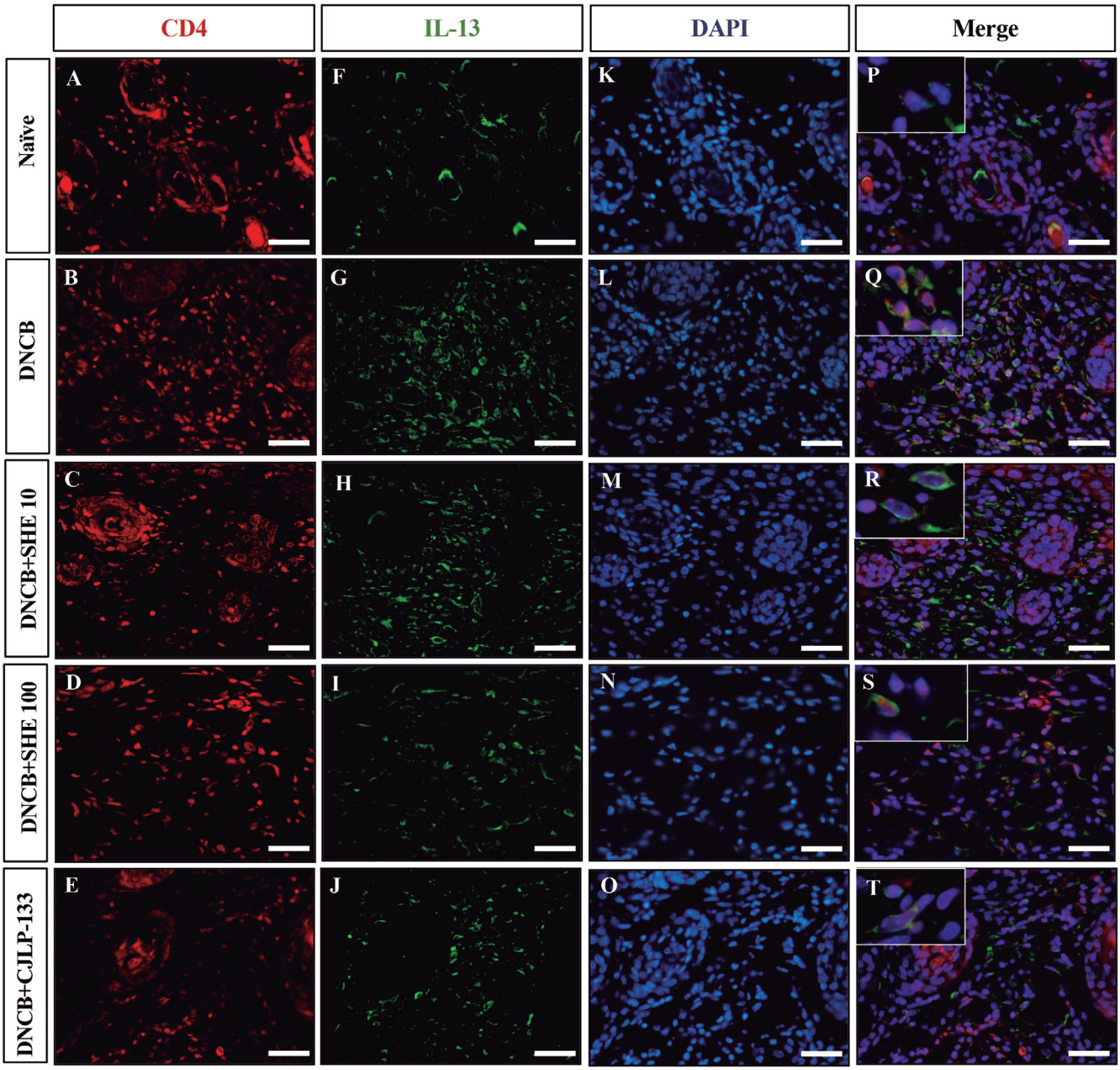

Fig. 5. SHE reduces IL-13 expression in the skin of DNCB-induced AD mice. Representative images of skin tissues for CD4 (red channel), IL-13 (green channel), and DAPI (blue channel) are shown. Images were merged to compare co-localization of CD4 and IL-13. Scale bars: 25 μm.

the level of mast cell infiltration and degranulation in skins of DNCB-induced AD mice.

SHE suppressed IL-13 expression on CD4⁺ T cells in the skin of DNCB-induced AD mice

To determine the effect of DNCB and SHE on the expression of IL-13, an archetypal phenotype marker of AD, in $CD4^+$ cells, fluorescent double immunostaining was performed on skins of DNCB-induced AD mice (Fig. 5). Cell nuclei were also stained using DAPI for better identification of cell organization in sections.

Composite fluorescent images clearly show the presence of a small population of $CD4^+$ (red) cells and those with high IL-13 (green) expression as well as their colocalization (purple) in skin tissues of the naïve group. However, the proportion of cells stained positive for CD4 and IL-13 in the DNCB group was larger than that

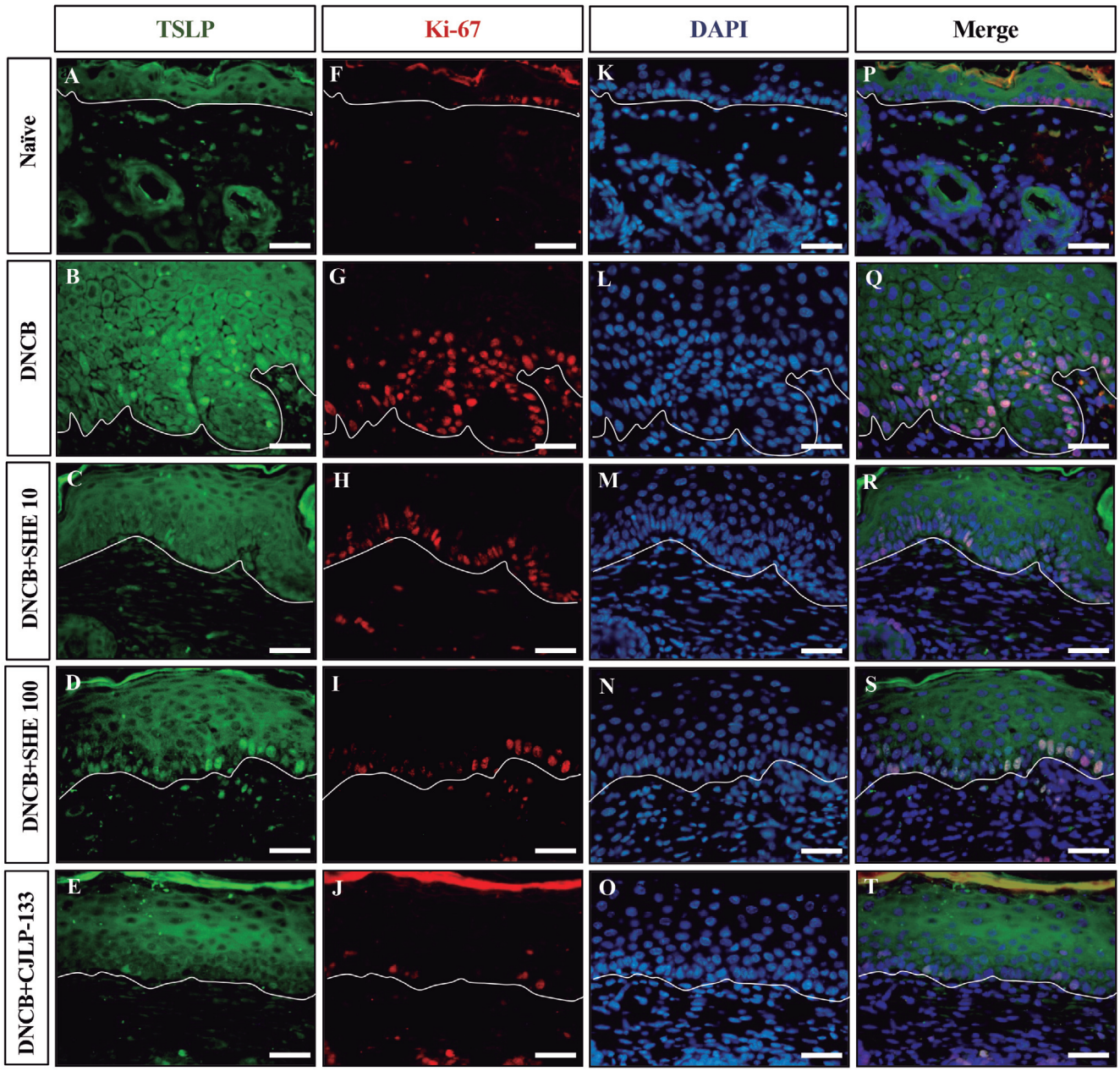

Fig. 6. SHE restricts the elevated TSLP expression in the skin of DNCB-induced AD mice. Representative images of skin tissues for TSLP staining (green channel), Ki-67 (red channel), and DAPI (blue channel) are shown. Images were merged to compare co-localization of CD4 and IL-13. White lines indicate boundary between epidermal and dermal layers. Scale bars: 25 μm.

in the naïve group as evidenced by the high number of cells in merged images in Fig. 5. Besides, in the DNCB group, when images of the same section were superimposed, most of the IL-13 positive cells were shown to be positive for CD4 as well. Interestingly, only a few cells were positive for both CD4 and IL-13 in the DNCB+SHE10 and DNCB+SHE100 groups, and similarly in the DNCB+CJLP133 group.

SHE lowered the expression of TSLP and Ki-67 in keratinocytes in the skin of DNCB- induced AD mice

TSLP expression in keratinocytes is normally induced in response to perturbations in skin structure or function. To determine the expression of TSLP in keratinocytes due to DNCB challenge and SHE treatment, we performed double immunofluorescence staining for TSLP (green) and Ki-67 (red), and the results are shown in Fig. 6. Here, nuclei were counterstained with DAPI (blue).

In skin tissues of the naïve group mice, only a very limited number of cells showed high expression of TSLP and Ki-67 (Fig. 6). Interestingly, cells expressing Ki-67 also expressed TSLP (purple; Fig. 6), but not all cells expressing TSLP expressed Ki-67. However, when DNCB was applied, the number of cells expressing TSLP and Ki-67 increased dramatically compared with that in the naïve group. Spatial distribution of cells is more intriguing: cells expressing TSLP filled up the whole epidermal layer, but cells co-expressing Ki-67 and TSLP seemed to align along the border between epidermal and dermal layers. When we treated DNCB-challenged cells with SHE, however, the expression of TSLP in epidermal cells and the number of Ki-67 expressing cells were significantly decreased in a dose-dependent manner: the higher the SHE concentration, the more distinct the reduction of TSLP and Ki-67 expression (Fig. 6). Besides, the expression of TSLP in epidermal cells and the number of Ki-67 expressing cells in the DNCB+CJLP133 group were also substantially decreased.

These data suggest that the SHE could suppress the expression of TSLP in DNCB-induced AD mice.

SHE improved filaggrin deficiency in skin tissues of DNCB-induced AD mice

Since filaggrin deficiency is known to play an important role in skin barrier dysfunction, we investigated its expression by performing immunohistochemistry analysis. As expected, when DNCB was applied, we observed that filaggrin level was decreased by 3.5 folds in skin tissues compared with that in the naïve group ($p < 0.05$; Fig. 7A,B). However, we observed its expression was substantially restored with SHE treatments: the expression of filaggrin was much higher in the DNCB+SHE10 and DNCB+SHE100 groups than that in the DNCB group by 1.4 folds (Fig. 7C,F) and 1.6 folds (Fig. 7D,F; $p<0.05$), respectively. Interestingly, SHE treatment of 100 mg/kg was as effective as that of positive control, CJLP-133 (Fig. 7E) in restoring the expression of filaggrin in skins of DNCB-induced AD mice. Collectively, these results support the hypothesis that SHE administration modulates skin barrier function recovery by upregulating the production of epidermal protein filaggrin.

SHE down-regulated the mRNA expression of IL-13 and TSLP in skin, and the levels of IgG_1 and IgG_{2a} in serum of DNCB-induced AD mice

When DNCB was applied, the mRNA expression of IL-13 and TSLP was significantly increased by 14 and 8 folds, respectively, compared to that in the naïve group (Fig. 8A,B). SHE treatment, however, significantly attenuated the mRNA expression of IL-13 in the DNCB+SHE 10 group by 14.7 folds ($p<0.005$) and the expression of TSLP by 4 folds ($p<0.05$) in DNCB+SHE 10 and DNCB+SHE 100 groups compared to that in the DNCB group, respectively. These data clearly suggest that SHE might be effective in mitigating DNCB-induced AD via suppressing TSLP and IL-13 in NC/Nga mice.

To determine if IgG's play a key role on the severity of AD skin barrier, we investigated the effect of SHE on the generation of IgG_1 and IgG_{2a}, separately. It is obvious that, when DNCB was applied, IgG_1 and IgG_{2a} levels were significantly increased (by 1.9 and 1.5 folds, respectively; $p<0.05$, Fig. 8C,D) compared to that in the naïve group. However, the level of IgG_1 seemed significantly decreased in the DNCB+SHE 100 and DNCB+CJLP-133 groups (by 1.5 and 1.9 folds; $p<0.005$) compared to that in the DNCB group, indicating the suppressive ability of SHE (Fig. 8C). As expected, significantly lower level of IgG_{2a} was also observed in DNCB+SHE 100 compared to that in the DNCB group (by 1.4 folds; Fig. 8D) as was observed in the positive control DNCB+CJLP-133 group (by 1.6 folds; Fig. 8D). These results indicate that the oral administration of SHE could effectively alleviate HDM/DNCB-induced AD-like skin lesions by suppressing the serum IgG_1 and IgG_{2a} levels.

Discussion

In this study, we examined the phenotypic changes incurred when DNCB induced AD-like symptoms in NC/Nga mice and evaluated the effect of SHE on attenuating them through promoting skin barrier function. DNCB was applied epicutaneously on dorsal skins of NC/Nga mice repeatedly to induce AD-like symptoms and skin lesions. However, SHE was treated orally since its active substances such as polyphenols and polysaccharides are readily absorbed early in digestion, and chromenes exhibit good absorption and metabolic stability to allow oral administration (Kazeem et al., 2013; Mateos et al., 2018).

Previous studies mentioned mast cell infiltration as a

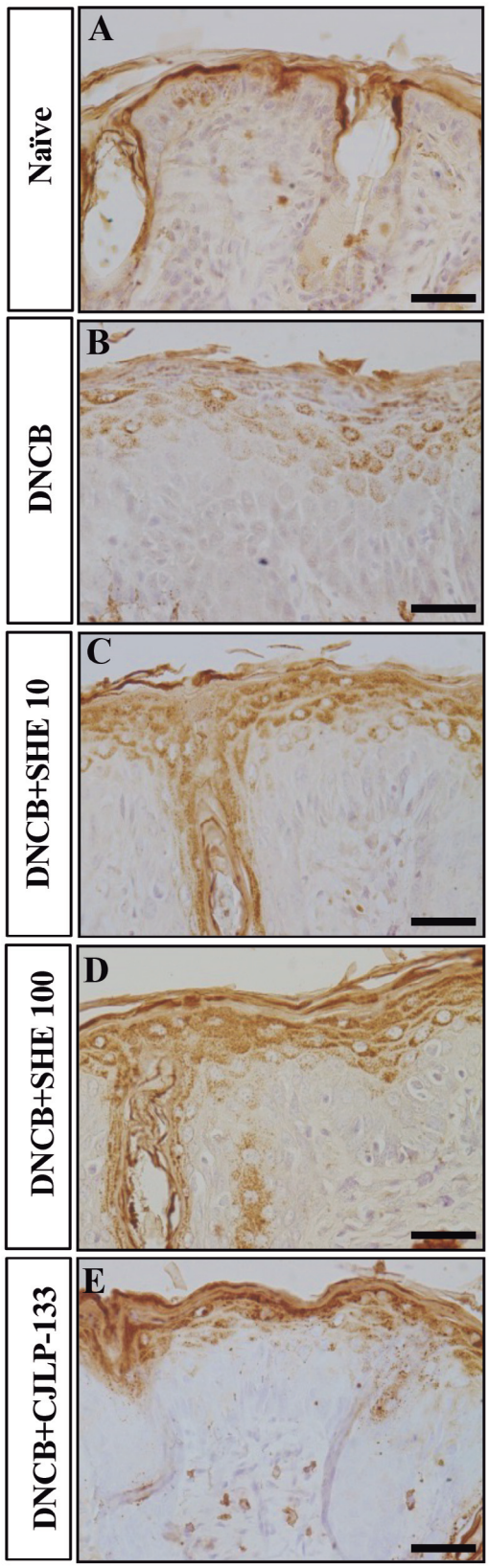

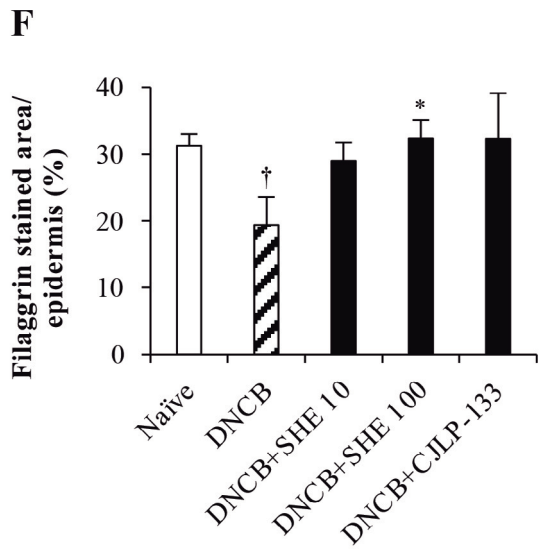

Fig. 7. SHE increased filaggrin expression in skins of DNCB-induced AD mice. **A-E.** Morphometric analysis of the filaggrin positive areas in mice skin epidermis against total areas of epidermis is displayed. **F.** Filaggrin stained area/epidermis (%) in skin is shown. Data are presented as the mean ± SE of changes in values. * ($p<0.05$) and ** ($p<0.005$) indicate significant increases compared to the naïve group, and † ($p<0.05$), †† ($p<0.005$) represent significant decreases compared to the DNCB group. Scale bars: 25 μm.

key character of AD lesions (Kim et al., 2012). In our study, we also observed an increased number of mast cells in the dermis in response to allergic inflammation when DNCB was applied, and it was reduced following SHE treatments. Histamine is one of the immune mediators released by mast cells and is known to be involved in inducing itchiness and edema in AD (Um and Jo, 2016). Also, high affinity of IgE to receptors on mast cells is known to cause their degranulation and to play a key role in inflammation (Kim et al., 2016). Our results demonstrated that SHE suppressed mast cell degranulation in skin, hinting at the possibility of SHE inhibiting mast cell infiltration and degranulation possibly via contraction of IgE.

Moreover, immune dysregulation predominantly due to disturbed Th2 cytokine balance has been interpreted as the main pathogenesis mechanism of AD. In particular, Th2 cytokines IL-4 and IL-13 have a permissive effect on microbial invasion and epidermal barrier disruption by inhibiting AMP production, reducing lipid production in the stratum corneum and inducing spongiosis. They downregulate the expression of the major EDC genes including filaggrin, loricrin and involucrin. They also stimulate keratinocytes to express TSLP, which serves as a crucial link between barrier defects and Th2 polarization (Kim et al., 2016). Of them, IL-13 has been suggested to be the master Th2 cytokine driving inflammation in the periphery. There is increasing evidence that this concept holds true for the inflammatory reaction underlying AD where IL-13 is overexpressed locally and has a significant impact on skin biology, including the recruitment of inflammatory cells, the alteration of the skin microbiome, and the impairment of the epidermal barrier function. More importantly, from an immunological point of view, high expression of TSLP, which coincides with enhanced IL-13 cytokine level that is characterized with fibrosis which leads to permanent and long-lasting damage in Th2 mediated inflammation is considered as a vital pathogenic factor in AD development (Cianferoni and Spergel., 2014). In our study, SHE treatment significantly reduced CD4 and IL-13 expression in skin compared to that in the DNCB group. And it is interesting to note that polyphenols also reduce B cell

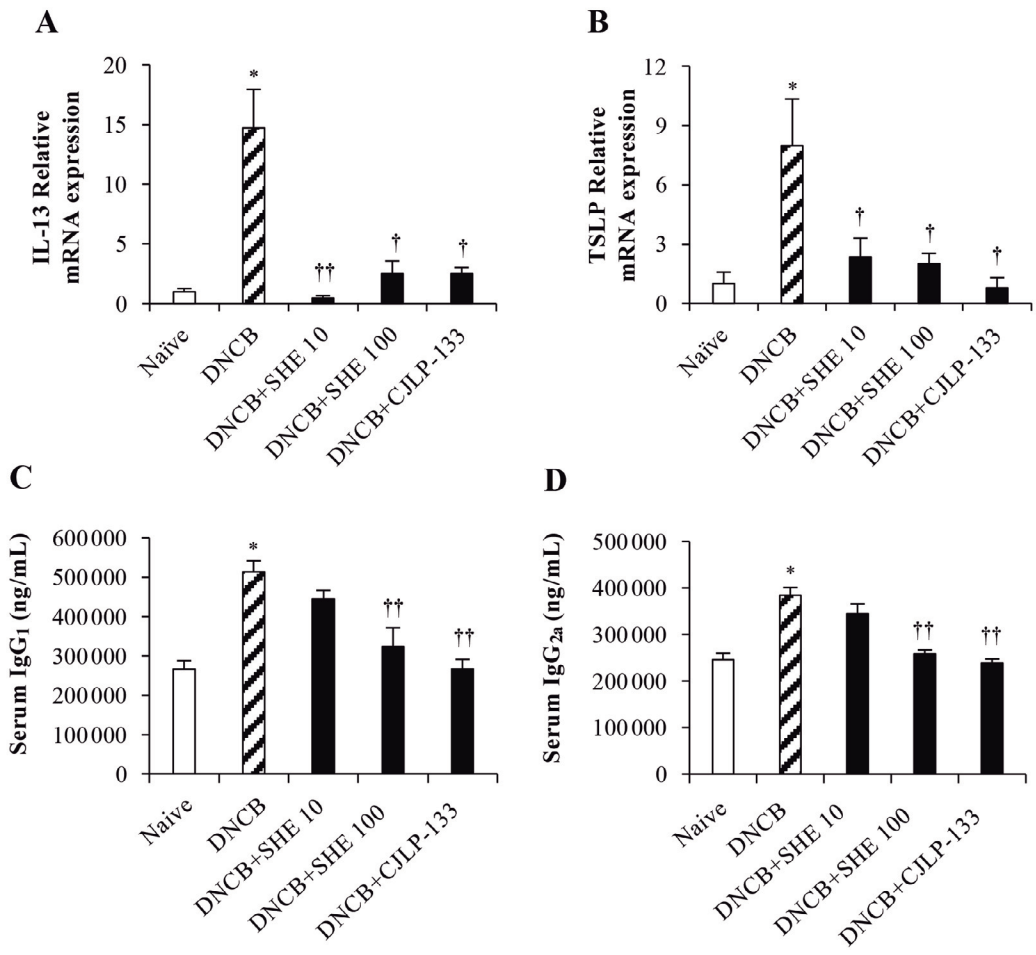

Fig. 8. SHE decreases the mRNA expression in skin and the levels of IgG_1 and IgG_{2a} in serum of DNCB-induced AD mice. Relative mRNA expression of **(A)** IL-13 and **(B)** TSLP in a skin normalized to the level of β-actin, and **(C)** serum IgG_1 and **(D)** IgG_{2a} levels of DNCB-induced mice are shown. Data are presented as the mean ± SE of changes in values. * ($p<0.05$) indicates a significant increase compared to the naïve group, and † ($p<0.05$) and †† ($p<0.005$) represent significant decreases compared to the DNCB group.

antibody and T cell cytokine production during allergen re-exposure (Witzel-Rollins et al., 2019), which might also play a role in SHE's anti-inflammatory efficacy observed in this study. Not only that, the role of IL-13 seems to be vital in AD as this promotes isotype switching in B cells, which subsequently results in the generation of IgG_1, a prominent factor for reducing skin barrier proteins. Moreover, in AD mice, functions of Th1 cells have a greater effect on enhancing the production of IgG_{2a} in B cells (Kim et al., 2020). Therefore, the serum IgG_1 and IgG_{2a} levels are known as a key factor for AD as it regulates the balance of Th1//Th2 (Shershakova et al., 2016). However, previous investigations reported that low level of IgG is obvious in non-atopic mild type asthma (Ercan et al., 2013) while a prominent drug, prednisolone, is able to suppress the production of IgG_1 and IgG_{2a} in an AD model (Kim et al., 2020). Moreover, a study showed that oral administration of SHE has a potential to downregulate the serum IgG_1 and IgG_{2a} levels in DNCB-induced mice and to decrease the severity of AD (Han et al., 2020). Validating these, our results clearly showed that SHE treatment significantly down-regulates the levels of IgG_1 and IgG_{2a} and has an inhibitory effect against AD on NC/Nga mice.

Since histological changes play a major role in chronic inflammatory diseases, histopathological analysis usually defines a fundamental baseline of phenotypic changes in AD. In this study, we observed that the epidermal thickness increased substantially in the DNCB group but was significantly reduced following the treatment with SHE, demonstrating the inhibition of inflammatory cells and the restoration of skin barrier function with SHE treatment. When we investigated the epidermal proliferation of AD skin using Ki-67 marker, we found an increase in epidermal proliferation in the DNCB group, suggesting disturbed differentiation (Proksch, 2009), and its reduction with SHE treatment, indicating SHE's potency to restore disrupted cellular proliferation control mechanism.

Moreover dysfunction of epidermal barrier in AD is closely accompanied with abnormal synthesis of structural proteins such as filaggrin (Furue et al., 2017; Pelc et al., 2018). In particular, filaggrin is considered as a major protein contributing to skin barrier formation and, according to previous studies, increased antigen penetration was seen in filaggrin-deficient mice (Kawasaki et al., 2012) and enhanced allergen penetration was observed when the skin barrier was defective (Kim et al., 2018b). When we determined filaggrin expression in skin tissues of DNCB-induced AD mice in this study, we found that SHE improved the skin barrier function by restoring filaggrin expression. The effect of SHE to improve the skin barrier function suggests that it can inhibit allergen-induced derangement of keratinocyte function.

Filaggrin deficiency in AD-like skin lesions increases the expression of TSLP, which in turn contributes highly to the development of further inflammation and aggravates AD-like lesions (Suyama et al., 2022) via activating dendritic cells and mast cells where inflammatory Th2 cells and cytokines are subsequently generated (Nagarkar et al., 2012; Kim et al., 2014; Pelc et al., 2018). However, SHE treatment reduced the number of TSLP positive cells and Th2 cytokine IL-13 in skins and ears of DNCB-induced AD mice, ameliorating skin lesions of AD. This posits SHE as a putative therapeutic agent for AD.

In this study, we investigated the effect of SHE against AD-like symptoms using an animal model where DNCB was applied epicutaneously to induce AD-like lesions on the skin of NC/Nga mice. In particular, we focused on the skin barrier function and observed that SHE treatment was able to restore proper skin barrier function disrupted by DNCB challenge via reestablishing the perturbed control mechanism of Th2 immune responses. We conclude that SHE has a therapeutic potential as an agent for treating AD by restoring skin barrier function that is compromised due to prolonged inflammation.

Acknowledgements and funding. This research is funded by Ministry of Oceans and Fisheries (Project No. 20150306) and the Ministry Education (Project No. 2019R1A6A1A10072987), Korea. We would like to thank Dr. T.H Chung for editorial assistance.
Competing interest. The authors declare that there are no conflicts of interest.

References

Bieber T. (2010). Atopic dermatitis. Ann. Dermatol. 22, 125-137.

Cianferoni A. and Spergel J. (2014). The importance of TSLP in allergic disease and its role as a potential therapeutic target. Expert Rev. Clin. Immunol.10, 1463-1474.

De Vuyst E., Salmon M., Evrard C., Lambert de Rouvroit C. and Poumay Y. (2017). Atopic dermatitis studies through in vitro models. Front. Med. 4, 119.

Ercan H., Ispir T., Kirac D., Baris S., Ozen A., Oztezcan S. and Cengizlier M.R. (2013). Predictors of atopic dermatitis phenotypes and severity: Roles of serum immunoglobulins and filaggrin gene mutation R501X. Allergol. Immunopathol. 41, 86-93.

Furue M., Chiba T., Tsuji G., Ulzii D., Kido-Nakahara M., Nakahara T. and Kadono T. (2017). Atopic dermatitis: immune deviation, barrier dysfunction, IgE autoreactivity and new therapies. Allergol. Int. 66, 398-403.

Han E.J., Fernando I.P.S., Kim H.S., Jeon Y.J., Madusanka D.M.D., Dias M.K.H.M., Jee Y. and Ahn G. (2020). Oral administration of *Sargassum horneri* improves the HDM/DNCB-induced atopic dermatitis in NC/Nga mice. Nutrients. 12, 1-14.

Herath K.H.I.N.M., Cho J., Kim A., Kim H.-S., Han E.J., Kim H.J., Kim M.S., Ahn G., Jeon Y.J. and Jee Y. (2019). Differential modulation of immune response and cytokine profiles of *Sargassum horneri* ethanol extract in murine spleen with or without Concanavalin A stimulation. Biomed. Pharmacother. 110, 930-942.

Herath K.H.I.N.M., Kim H.J., Lee J.H., Je J.G., Yu H.-S., Jeon Y.-J., Kim H.J. and Jee Y. (2021). *Sargassum horneri* (Turner) C. Agardh containing polyphenols attenuates particulate matter-induced

inflammatory response by blocking TLR-mediated MYD88-dependent MAPK signaling pathway in MLE-12 cells. J. Ethnopharmacol. 265, 113340.

Jeong D.-H., Kim M.-J., Kang B.-K. and Ahn D.-H. (2014). Anti-inflammatory activity of methanol extract and N-hexane fraction mojabanchromanol b from *Myagropsis myagroides*. Life Sci. 114, 12-19.

Kantor R. and Silverberg J.I. (2017). Environmental risk factors and their role in the management of atopic dermatitis. Expert Rev. Clin. Immunol. 13, 15-26.

Kawasaki H., Nagao K., Kubo A., Hata T., Shimizu A., Mizuno H., Yamada T. and Amagai M. (2012). Altered stratum corneum barrier and enhanced percutaneous immune responses in filaggrin-null mice. J. Allergy Clin. Immunol. 129, 1538-1546. e1536.

Kazeem M.I., Akanji M.A., Yakubu M.T. and Ashafa A.O.T. (2013). Protective effect of free and bound polyphenol extracts from ginger *(Zingiber officinale* Roscoe) on the hepatic antioxidant and some carbohydrate metabolizing enzymes of streptozotocin-induced diabetic rats. Evid. Based Complement. Alternat. Med. 2013, 935486.

Kim H.-S., Sanjeewa K., Fernando I., Ryu B., Yang H.-W., Ahn G., Kang M.C., Heo S.-J., Je J.-G. and Jeon Y.-J. (2018a). A comparative study of *Sargassum horneri* Korea and China strains collected along the coast of Jeju Island South Korea: its components and bioactive properties. Algae 33, 341-349.

Kim H., Kim J.R., Kang H., Choi J., Yang H., Lee P., Kim J. and Lee K.W. (2014). 7, 8, 4 Trihydroxyisoflavone attenuates DNCB-induced atopic dermatitis-like symptoms in NC/Nga mice. PLoS One 9, e104938.

Kim J.E., Kim J.S., Cho D.H. and Park H.J. (2016). Molecular mechanisms of cutaneous inflammatory disorder: atopic dermatitis. Int. J. Mol. Sci. 17, 1234.

Kim S.H., Seong G.S. and Choung S.Y. (2020). Fermented *Morinda citrifolia* (Noni) alleviates DNCB-induced atopic dermatitis in NC/Nga mice through modulating immune balance and skin barrier function. Nutrients 12, 1-18.

Kim T.-H., Kim G.-D., Jin Y.-H., Park Y.S. and Park C.-S. (2012). Omega-3 fatty acid-derived mediator, Resolvin E1, ameliorates 2, 4-dinitrofluorobenzene-induced atopic dermatitis in NC/Nga mice. Int. Immunopharmacol. 14, 384-391.

Kim Y.-J., Choi M.J., Bak D.-H., Lee B.C., Ko E.J., Ahn G.R., Ahn S.W., Kim M.J., Na J. and Kim B.J. (2018b). Topical administration of EGF suppresses immune response and protects skin barrier in DNCB-induced atopic dermatitis in NC/Nga mice. Sci. Rep. 8, 1-11.

Kolb L. and Ferrer-Bruker S.J. (2020). Atopic dermatitis StatPearls. Treasure Island (FL): StatPearls Publishing Copyright© 2020, StatPearls Publishing LLC.

Lee S.H., Heo Y. and Kim Y.C. (2010). Effect of German chamomile oil application on alleviating atopic dermatitis-like immune alterations in mice. J. Vet. Sci. 11, 35-41.

Mateos A.G., Palomino J.C., Clauzel L.M. and Carulla D.T. (2018). Chromene derivatives as inhibitors of TCR-Nck interaction: Google Patents.

Nagarkar D.R., Poposki J.A., Comeau M.R., Biyasheva A., Avila P.C., Schleimer R.P. and Kato A. (2012). Airway epithelial cells activate TH2 cytokine production in mast cells through IL-1 and thymic stromal lymphopoietin. J. Allergy Clin. Immunol.130, 225-232.e24.

Pelc J., Czarnecka-Operacz M. and Adamski Z. (2018). Structure and function of the epidermal barrier in patients with atopic dermatitis–treatment options. Part one. Postepy Dermatol. Alergol. 35, 1.

Proksch E. (2009). Protection against dryness of facial skin: a rational approach. Skin Pharmacol. Physiol. 22, 3-7.

Ray R.J., Furlonger C., Williams D.E. and Paige C.J. (1996). Characterization of thymic stromal-derived lymphopoietin (TSLP) in murine B cell development in vitro. Eur. Immunol. 26, 10-16.

Sanjeewa K.A., Jayawardena T.U., Kim H.-S., Kim S.-Y., Ahn G., Kim H.-J., Fu X., Jee Y. and Jeon Y.-J. (2019). Ethanol extract separated from *Sargassum horneri* (Turner) abate LPS-induced inflammation in RAW 264.7 macrophages. Fish. Aquatic Sci. 22, 1-10.

Shershakova N., Baraboshkina E., Andreev S., Purgina, D., Struchkova I., Kamyshnikov O., Nikonova A. and Khaitov M. (2016). Anti-inflammatory effect of fullerene C60 in a mice model of atopic dermatitis. J. Nanobiotechnology 14, 1-11.

Suyama P., Dinh D., Cho J., Herath K., Kim H., Ko O., Jeon Y., Ahn G. and Jee J. (2022). Polyphenol-rich *Sargassum horneri* alleviates atopic dermatitis-like skin lesions in NC/Nga mice by suppressing Th-2 mediated cytokine IL-13. (Submitted).

Um Y.L. and Jo Y.W. (2016). Inhibitory effects of *Calophyllum inophyllum* extract on atopic dermatitis induced by DNCB in mouse. Am. J. Phytomed. Clin. Therap. 4, 165-173.

Wijesinghe W. and Jeon Y.-J. (2011). Biological activities and potential cosmeceutical applications of bioactive components from brown seaweeds: a review. Phytochem. Rev. 10, 431-443.

Witzel-Rollins A., Murphy M., Becvarova I., Werre S.R., Cadiergues M.-C. and Meyer H. (2019). Non-controlled, open-label clinical trial to assess the effectiveness of a dietetic food on pruritus and dermatologic scoring in atopic dogs. BMC Vet. Res. 15, 1-10.

Zheng T., Oh M.H., Oh S.Y., Schroeder J.T., Glick A.B. and Zhu Z. (2009). Transgenic expression of interleukin-13 in the skin induces a pruritic dermatitis and skin remodeling. J. Invest. Dermatol. 129, 742-751.

Accepted May 30, 2022